Proteolytic cleavage of the extracellular domain affects signaling of parathyroid hormone receptor 1

1 **Christoph Klenk[1,#*], Leif Hommers[2,3,4], Martin J. Lohse[1,5,6,7]**

2 [1]Institute of Pharmacology and Toxicology, University of Würzburg, Würzburg, Germany
3 [2]Interdisciplinary Center for Clinical Research, University Hospital of Würzburg, Würzburg,
4 Germany
5 [3]Department of Psychiatry, Psychosomatics and Psychotherapy, Center for Mental Health,
6 University Hospital of Würzburg, Würzburg, Germany.
7 [4]Comprehensive Heart Failure Center (CHFC), University Hospital of Würzburg, Würzburg,
8 Germany.
9 [5]Rudolf Virchow Center, University of Würzburg, Würzburg, Germany
10 [6]Max Delbrück Center for Molecular Medicine (MDC), Berlin, Germany
11 [7]ISAR Bioscience Institute, Planegg, Germany
12 [#]present address: Department of Biochemistry, University of Zurich, Zurich, Switzerland
13

14 * Corresponding author: Christoph Klenk, c.klenk@bioc.uzh.ch
15

Abstract

Parathyroid hormone 1 receptor (PTH1R) is a member of the class B family of G protein-coupled receptors, which are characterized by a large extracellular domain required for ligand binding. We have previously shown that the extracellular domain of PTH1R is subject to metalloproteinase cleavage *in vivo* that is regulated by ligand-induced receptor trafficking and leads to impaired stability of PTH1R. In this work, we localize the cleavage site in the first loop of the extracellular domain using amino-terminal protein sequencing of purified receptor and by mutagenesis studies. We further show, that a receptor mutant not susceptible to proteolytic cleavage exhibits reduced signaling to G_s and increased activation of G_q compared to wild-type PTH1R. These findings indicate that the extracellular domain modulates PTH1R signaling specificity, and that its cleavage affects receptor signaling.

Introduction

Parathyroid hormone 1 receptor (PTH1R) is a key regulator of blood calcium levels and bone metabolism in response to parathyroid hormone (PTH). Moreover, activation of PTH1R by parathyroid-related hormone peptide (PTHrP) has been implicated in fetal development and in malignancy-associated hypercalcemia (1). PTH1R is a member of the class B family of G protein-coupled receptors (GPCRs) which are characterized by a large N-terminal extracellular domain (ECD; ~100 to 180 residues) that is critically involved in ligand binding (2,3). Similar to other class B GPCRs, the ECD of PTH1R consists of two pairs of antiparallel β-strands flanked by a long and a short α-helical segment at the N- and C-terminal end, respectively. The overall conformation is constrained by three conserved disulfide bonds which are required for proper folding and for ligand binding (4-7). The ECD is oriented in an upright position above the membrane surface with residues 15-34 of PTH binding into a groove formed by the ECD and the N-terminal part of the ligand protrudes as a continuous α-helix into the transmembrane domain of PTH1R (Fig. 1) (7). In line with the receptor structure, a two-step activation model has been proposed, where first the C-terminal part of PTH binds to the extracellular domain, and then the N-terminal part of PTH interacts with the receptor core, thereby leading to receptor activation (8,9). PTH1R couples to multiple heterotrimeric G protein subtypes and can activate several signaling pathways concomitantly. Predominantly, adenylyl cyclases are stimulated by activation of G_s as well as phospholipase Cβ by G_q (10-12). Moreover, activation of $G_{i/o}$ resulting in inhibition of adenylyl cyclase and activation of $G_{12/13}$ leading to phospholipase D and RhoA activation, as well as activation of mitogen-activated protein kinases through G protein-dependent and -independent mechanisms

have been reported (13-18). PTH1R activation can have anabolic and catabolic effects on bone. While continuous administration of PTH enhances osteoclastogenesis leading to bone resorption and calcium liberation, intermittent administration of PTH results in bone formation through enhancing osteoblast differentiation and survival, which is used as a treatment option for severe osteoporosis (19,20). Although the exact molecular mechanisms are not clear yet, differential activation of signaling pathways seems to play an important role in these opposing effects upon PTH1R activation. While G_s-signaling is the predominant pathway for promoting PTH-induced bone formation, G_q-activation seems to have little or no effect on osteogenesis (21-23). In addition, β-arrestin recruitment was shown to be essential for selectively promoting bone formation upon treatment of mice with recombinant PTH(1-34) (24). Moreover, many of these effects appear to be regulated in a tissue- and cell-type specific manner (25).

We have previously shown that the ECD of PTH1R can undergo proteolytic cleavage by an extracellular metalloproteinase resulting in reduced stability and degradation of the receptor. We also demonstrated that N-terminal ECD cleavage occurred only at the cell surface, and that internalization of the receptor resulting from continuous activation by agonists prevented cleavage and thereby stabilized the receptor. Furthermore, our experiments suggested that the cleavage site is located within the first 90 residues of the receptor, however the exact position was not fully resolved (26). In the present study, we have localized the cleavage site in the unstructured loop of exon E2 within the PTH1R ECD. Moreover, we demonstrate that ECD cleavage results in an altered ligand efficacy of PTH changing the G protein-coupling of PTH1R from G_q to G_s.

Materials and Methods

Materials

Lipofectamine 2000 was purchased from Thermo Fisher Scientific. [$Nle^{8,18}$,Tyr^{34}]PTH (1-34), a chemically more stable variant of native PTH, was purchased from Bachem and is referred to as PTH(1-34). Generation of a polyclonal rabbit anti-PTH1R (1781) antiserum was described previously (27). Anti-rabbit peroxidase-conjugated secondary antibodies were obtained from Dianova. Cy2-conjugated anti-rabbit antibody was from Jackson Immuno Research Lab. All cell culture media were obtained from PAN Biotech. All other reagents were of analytical grade from Sigma-Aldrich or Applichem.

81 **cDNA constructs**

82 A Strep-Tag II (WSHPQFEK) was fused to the C-terminal end of human PTH1R (26) by
83 PCR. Alanine mutations were introduced into the extracellular domain of PTH1R by overlap
84 extension PCR. In total, 6 constructs with alanine blocks from Leu^{56}-Met^{63}, Glu^{64}-Ser^{71},
85 Ala^{72}-Arg^{79}, Lys^{80}-Leu^{87}, Tyr^{88}-Lys^{95}, and Glu^{96}-Tyr^{103} were generated. All constructs were
86 subcloned into pcDNA5/FRT vector (Thermo Fisher Scientific) using the restriction sites
87 EcoRI and ApaI and verified by sequencing.

88 **Cell culture and transfection**

89 Flp-In CHO cells (Thermo Fisher Scientific) were maintained in 1:1 Dulbecco's modified
90 Eagle's medium/ Ham's F12 medium containing 10 % (v/v) fetal calf serum, 100 U/ml
91 penicillin, 100 µg/ml streptomycin and 100 µg/ml Zeocin (Thermo Fisher Scientific). Cells
92 were maintained at 37 °C in a humidified atmosphere of 5% CO_2, 95% air. To generate stable
93 cell lines, cells were transfected with pcDNA5/FRT-PTH1R plasmids using Lipofectamine
94 2000 according to the manufacturer's instructions. 48 h after transfection, cells were selected
95 in culture medium where Zeocin was replaced by 600 µg/ml hygromycin B for approximately
96 two weeks. Clonal cell lines were derived from limited dilution series and screened for
97 expression of PTH1R by Western blot and immunocytochemistry.

98 **SDS-PAGE and Western blotting**

99 Cells were lysed in SDS-loading buffer [50 mM Tris (pH 6.8), 2% (v/v) SDS, 10% glycerol, 5
100 mg/ml bromophenol blue] for 20 min on ice, briefly sonified and incubated at 45 °C for 20
101 min. For reducing conditions, 4% (v/v) β-mercaptoethanol was added to the lysis buffer.
102 Lysates were cleared by centrifugation and run on 10% SDS-polyacrylamide gels in a Mini-
103 PROTEAN 3 cell apparatus (Biorad). Proteins were electroblotted onto Immobilon P
104 membranes (Millipore) using a Bio-Rad Mini trans-blot cell apparatus at 100 V for 60 min at
105 4 °C. The blots were probed with anti-PTH1R antibodies (1:4,000), followed by horseradish
106 peroxidase-conjugated goat anti-rabbit (1:10,000) and detection on Super RX X-ray film
107 (Fujifilm) using ECL Plus reagent (GE Healthcare).

108 **Purification of PTH1R**

109 Membranes from Flp-In CHO cells stably expressing PTH1R-Strep2 were prepared as
110 described before (28). Membranes were solubilized in solubilization buffer [50 mM Tris-HCl
111 (pH 7.4), 140 mM NaCl, 0.5% (w/v) n-dodecyl β-D-maltoside, 10 µg/ml soybean trypsin
112 inhibitor, 30 µg/ml benzamidine, 5 µg/ml leupeptin, 100 µM PMSF] for 2 h, and insoluble
113 material was removed by centrifugation for 1 h at 100,000 × g. Solubilized PTH1R-Strep2

114 was incubated with 1 ml Strep-Tactin sepharose (IBA GmbH) for 12 h under constant
115 agitation and washed with 10 column volumes of wash buffer [100 mM Tris-HCl (pH 8.0),
116 1 mM EDTA, 150 mM NaCl, 0.1% (w/v) n-dodecyl β-D-maltoside]. Bound receptor was
117 eluted with 1-2 column volumes of the same buffer supplemented with 2.5 mM desthiobiotin
118 and concentrated with a Microcon centrifugal filter device (10,000 MWCO, Millipore).

119 **Amino-terminal sequencing of cleaved receptor fragments**

120 Fifty µg of purified receptor fragments were blotted onto PVDF membranes and stained with
121 Coomassie Blue. The fragments were excised and subjected to automated Edman degradation
122 (Wita GmbH).

123 **Immunocytochemistry and confocal imaging**

124 CHO cells stably expressing PTHR variants were grown on coverslips overnight. Cells were
125 then exposed (or not) to 100 nM PTH(1-34) for 30 min as indicated. Cells were fixed with 4%
126 paraformaldehyde and 0.2% picric acid in 0.1 M phosphate buffer (pH 6.9) for 30 min at
127 room temperature and washed five times in PBS. For permeabilization cells were incubated
128 for 5 min in methanol. After 10 min of preincubation in PBS containing 0.35% (w/v) BSA,
129 cells were incubated with anti-PTH1R antibody at a dilution of 1:2,000 in PBS containing
130 0.35% (w/v) BSA for 1 h at 37 °C. Bound primary antibody was detected with Cy2-labeled
131 goat anti-rabbit IgG (1:400). Specimens were examined using a Leica SP2 laser scanning
132 confocal microscope.

133 **Functional receptor assays**

134 Signaling assays were measured in Flp-In CHO cells stably expressing the indicated PTH1R
135 variants. cAMP was measured using a RIA kit (Beckman Coulter), and inositol phosphates
136 were separated by chromatographic separation of myo-[2-^{3}H]inositol phosphates as described
137 previously (29). Pharmacological data were analyzed in Prism v6.0 (GraphPad Software). A
138 three-parameter logistic equation was fit to the data to obtain concentration-response curves
139 and E_{max} values. Statistical differences were analyzed using unpaired t-tests.

140 Results

141 Our previous findings suggested that the protease cleavage site is most likely located between
142 Cys^{48} and Cys^{108} (26), a region including exon E2 of PTH1R which is unique among all other
143 class B GPCRs and which forms a disordered loop in the crystal structures of the isolated
144 PTH1R ECD (4) and full length PTH1R (7) (Fig. 1). We therefore created a series of mutants
145 where stretches of 8 residues in this region were mutated to Ala to delineate the protease

146 cleavage site (Fig. 2A). Each of the six resulting PTH1R variants was stably expressed in
147 Flp-In CHO cells, and expression and membrane targeting of the receptor were analyzed by
148 immunofluorescence (Fig. 2B) using an antibody detecting the C-terminal part of PTH1R
149 (26,27). All mutants exhibited a distinct membrane staining which was comparable to that of
150 wild-type receptor. Upon stimulation with 100 nM PTH(1-34) for 30 min, a sequestration of
151 receptor from the cell surface into endocytic vesicles was observed suggesting that each
152 receptor variant activated intracellular signaling pathways leading to receptor internalization.

153 To test whether any of the mutations had an effect on protease cleavage, the migration
154 patterns of PTH1R variants were analyzed by reducing SDS-PAGE and Western blotting. As
155 demonstrated previously, the ECD of PTH1R residing at the cell surface is cleaved by
156 extracellular metalloproteinases. The resulting N-terminal fragment of the ECD (~10 kDa)
157 remains tethered to the receptor core by a single disulfide bond under native conditions but is
158 lost under reducing conditions leading to an apparent molecular weight of the receptor of ~80
159 kDa (26). In contrast, sustained receptor activation by PTH(1-34) resulting in continuous
160 receptor internalization rendered the receptor inaccessible for extracellular proteases and thus
161 protected the full-length receptor with a molecular weight of ~90 kDa (Fig 2C, left panel; c.f.
162 (26)). Similar to wild-type PTH1R, mutants where residues 64-71, 80-87, 88-95 or 96-103
163 had been replaced by alanines migrated at ~80 kDa in reducing SDS-PAGE, indicating that
164 protease cleavage was not prevented by the respective mutations. In contrast, $PTH1R^{56-63A}$
165 exclusively migrated at ~90 kDa similar to wild-type receptor where cleavage had been
166 prevented by stimulation with PTH(1-34). For $PTH1R^{72-79A}$ two bands were detected which
167 co-migrated with the cleaved and non-cleaved receptor species. Thus, mutating the region
168 between Leu^{56} and Met^{63} to alanine fully inhibited proteolytic cleavage of the PTH1R ECD,
169 indicating that the main cleavage site is located in this region. $PTH1R^{72-79A}$ exhibited
170 incomplete inhibition of cleavage, suggesting another, less susceptible cleavage site or an
171 incomplete masking of the cleavage site around residues 56-63.

172 To corroborate these findings, we determined the amino acid sequence of the N-terminus of
173 the cleaved 80 kDa fragment of PTH1R. PTH1R was purified from stably expressing Flp-In
174 CHO cells via a C-terminal Strep2 tag. 50 µg of purified protein were blotted onto PVDF
175 membrane and stained with Coomassie blue. A band corresponding to the cleaved PTH1R
176 fragment was excised and analyzed by Edman degradation (Fig. 3A). Three different N-
177 termini were identified, located at positions Ser^{65}, Ser^{73} and Lys^{80} in the ECD of PTH1R (Fig.
178 3B). Finally, the complete ECD of PTH1R (residues 23-177) was subjected to a

179 computational cleavage site search using positional weight matrices (PWM) for 11 matrix
180 metalloproteinases (MMPs) (30). This procedure revealed a total of 19 putative cleavage sites
181 located between residues 30 to 173. However, only cleavage site $Ser^{61}\downarrow Ile^{62}$ was common to
182 all 11 MMPs and exhibited the highest PWM scores among all other predicted cleavage sites
183 (Table 1). Taken together, these findings support the results of the alanine scan, suggesting
184 that the primary cleavage occurs at $Ser^{61}\downarrow Ile^{62}$ of PTH1R.

185 To test whether ECD cleavage affected receptor function, we assessed activation of the two
186 canonical signaling pathways of PTH1R G_s (cyclic AMP, cAMP) and G_q (inositol phosphates,
187 IP) by wild-type PTH1R, by the fully cleavage-deficient mutant $PTH1R^{56\text{-}63A}$, and by the
188 partially cleaved mutant $PTH1R^{72\text{-}79A}$. All measurements were performed in stably expressing
189 CHO cells that had been matched for equal receptor expression levels. Compared to wild-type
190 PTH1R, maximal PTH-induced generation of cAMP was reduced by 37% for $PTH1R^{56\text{-}63A}$,
191 whereas no change was observed for $PTH1R^{72\text{-}76A}$ (Fig. 4A, Table 2). In contrast, PTH-
192 induced generation of $[^3H]IP$ was increased by 35% for $PTH1R^{56\text{-}63A}$, whereas no change was
193 observed for $PTH1R^{72\text{-}79A}$ (Fig. 4B, Table 2). In summary, these findings suggest, that full
194 cleavage of the ECD of PTH1R leads to decreased efficacy of PTH(1-34) in G_q signaling and
195 increased efficacy in G_s signaling. $PTH1R^{72\text{-}79A}$ did not differ from wild-type PTH1R, which
196 may be explained by the fact that the majority of $PTH1R^{72\text{-}79A}$ was still proteolytically
197 processed (Fig. 3B). Thus, cleavage appears to directly modulate the signaling bias of
198 PTH1R.

199 Discussion

200 Previously, we have reported that the ECD of PTH1R is subject to cleavage by
201 metalloproteinases. PTH1R cleavage is a constitutive phenomenon and is inhibited by
202 receptor activation (26). In the present study we aimed to characterize the role of proteolytic
203 processing of the extracellular domain, and we provide evidence for the exact location of the
204 cleavage site as well as for a modulation of signaling properties upon cleavage. N-terminal
205 sequencing of the 80 kDa receptor core (remaining after shedding the cleaved N-terminal
206 fragment by disulfide hydrolysis) revealed three nearby cleavage sites ($Glu^{64}\downarrow Ser^{65}$,
207 $Ala^{72}\downarrow Ser^{73}$ and $Arg^{79}\downarrow Lys^{80}$). However, computational analysis using cleavage patterns of 11
208 MMPs suggested a putative cleavage site at $Ser^{61}\downarrow Ile^{62}$ which was located 3 amino acids
209 upstream of the first free N-terminus identified by microsequencing. A systematic alanine
210 scan within this region of the ECD showed, that only $PTH1R^{56\text{-}63A}$ was completely resistant to

211 proteolysis, while mutation of residues 64-71 to alanine did not prevent proteolysis, further
212 supporting the proximal site at residue 61. Only a fraction of PTH1R^{72-79A} remained intact
213 whereas the majority of receptor was found as the cleaved 80 kDa form. This may suggest,
214 that the alanine mutations at residues 72-79 mask the cleavage site around residues 56-63 to
215 some extent or may hamper protease interaction resulting in incomplete protease cleavage.
216 Considering the results from computational and biochemical analyses, we propose that
217 Ser^{61}↓Ile^{62} is the most likely primary cleavage site. The free N-termini observed in Edman
218 degradation at Ser^{65}, Ser^{73} and Lys^{80} may be the result of limited exopeptidase action
219 following endopeptidase cleavage. Ser^{61} is located within the first residues of a large loop
220 connecting the top layer formed by α1-helix with the first β-strand of the middle layer of the
221 α-β-β-α fold of PTH1R ECD. Notably, residues 61-104 were not resolved in any structure of
222 PTH1R-ECD or full length PTH1R suggesting high flexibility in this region (4,7,31).
223 Considering the orientation of the ECD in the full-length structures, Ser^{61} would be located at
224 the distal part of the receptor facing away from the membrane and, thus, may be well
225 accessible for extracellular proteases (Fig 1).

226 Processing by MMPs and other metalloproteinases has been described previously for a limited
227 number of other GPCRs, e.g. for β_1-adrenergic receptor (32), endothelin B receptor (33,34),
228 thyrotropin receptor (35,36), protease-activated receptor 1 (PAR-1) (37,38), GPR124 (39) and
229 more recently for GPR37 (40,41). Apart from PAR-1 and the adhesion family receptor
230 GPR124, where protease cleavage unmasks the endogenous ligand resulting in receptor
231 activation, a functional consequence of protease cleavage has not been explicitly reported. To
232 our surprise, proteolytic cleavage of the PTH1R ECD directly affected receptor signaling. In
233 contrast to wild-type receptor, the cleavage-deficient mutant PTH1R^{56-63A} exhibited reduced
234 cAMP and increased IP responses to PTH stimulation. Protease cleavage thus enhanced
235 coupling efficacy of the receptor to the G_s pathway, while reducing G_q-coupling at the same
236 time, resulting in a signaling bias. Biased signaling is defined as ligands giving different
237 degrees of activation in separate signaling pathways of the same receptor. Besides binding of
238 ligands to allosteric sites on the receptor that stabilize distinct active receptor conformations,
239 interaction of a receptor with intracellular adaptor proteins and subcellular receptor
240 sequestration have been reported to affect signaling bias (42-44). For PTH1R, several ligands
241 and intracellular adaptors which direct signaling specificity to G_s, G_q or G protein-
242 independent pathways have been described (17,22,24,45-48). All of these PTH/PTHrP
243 derivatives carry modifications at the N-terminal part, which directly interacts with the
244 transmembrane domain of the receptor, suggesting that signaling specificity is mediated by

245 direct conformational stabilization of the receptor core. Our findings now indicate that the
246 ECD, which accommodates the C-terminal part of PTH and which is commonly believed to
247 only serve as an "affinity trap" for the ligand, can also affect signaling specificity of the
248 receptor.

249 There is growing evidence, that extracellular regions of GPCRs play important roles in fine-
250 tuning receptor activity and signaling selectivity. Apart from PARs and adhesion receptors,
251 where the buried ligand is proteolytically released from the receptor's N-terminus,
252 extracellular loops play an important role in modulating the function of several class A and
253 class B receptors (49). More importantly, calcium-mediated interaction of extracellular loop 1
254 and PTH has been shown to modulate PTH1R activity (50-52). Recent studies on glucagon
255 receptor suggest that the ECD itself may act as an allosteric inhibitor by interaction of α1-
256 helix of the ECD with extracellular loop 3 of the receptor core (53). Moreover, recent cryo-
257 EM structures of active-state class B GPCRs including PTH1R reveal a high degree of
258 conformational flexibility of the ECD (31,54,55), and it has been proposed that the dynamic
259 motion of the ECD may contribute to biased agonism of class B GPCR ligands (56,57). In
260 line with that, an antibody primarily binding to α1-helix of the ECD has been shown to
261 modulate β-arrestin signaling of PTH1R (58) suggesting that perturbation of ECD orientation
262 or conformation may alter receptor signaling. Proteolytic cleavage at Ser^{61} is expected to
263 result in increased conformational flexibility of α1-helix of PTH1R ECD as the helix remains
264 tethered to the receptor only through a disulfide bond between Cys^{48} and Cys^{117}(26). As a
265 consequence, especially the N-terminal part of α1-helix may gain additional flexibility (Fig.
266 1). Notably, within this region residues 32-41 make important contacts to PTH including the
267 flexible central region of the peptide (Fig. 5) (4,7). This region was shown to be critical for
268 initiating the two-step binding mechanism of PTH (59). Thus, it may well be conceivable that
269 alterations in the flexibility and orientation of α1-helix of PTH1R ECD can allosterically
270 affect receptor signaling. Whether these effects are mediated by an altered interaction of the
271 ECD with the transmembrane core, by a rearrangement of the ligand in the binding pocket, or
272 involve interaction of additional proteins such as RAMPs (receptor activity-modifying
273 proteins) with PTH1R (60,61) needs to be studied.

274 In summary, we have mapped the cleavage site within the ECD of PTH1R and demonstrate
275 for the first time, to our knowledge, that protease cleavage of the ECD of a GPCR modulates
276 G protein signaling specificity.

Conflict of Interest

The authors declare that the research was conducted in the absence of any commercial or financial relationships that could be construed as a potential conflict of interest.

Author Contributions

CK and MJL conceived the study; CK designed experiments; CK and LH performed experiments; CK, LH and MJL analyzed data; CK wrote the manuscript, all authors provided edits and comments.

Funding

These studies were supported by grants from the Deutsche Forschungsgemeinschaft (SFB487) and the European Research Council (Advanced Grant TOPAS, No. 232944) to MJL.

Acknowledgments

We thank Michaela Hoffmann, Annette Hannawacker, Alexandra Bohl and Monika Frank for technical assistance. Moreover, we thank Dr. Thomas Pohl (Wita GmbH, Berlin) for support with N-terminal microsequencing.

291 **References**

292 1. Jüppner H, Abou-Samra AB, Uneno S, Gu WX, Potts JT, Segre GV. The parathyroid
293 hormone-like peptide associated with humoral hypercalcemia of malignancy and
294 parathyroid hormone bind to the same receptor on the plasma membrane of ROS 17/2.8
295 cells. *J Biol Chem* (1988) **263**:8557–8560.

296 2. Fredriksson R, Lagerström MC, Lundin L-G, Schiöth HB. The G-protein-coupled
297 receptors in the human genome form five main families. Phylogenetic analysis,
298 paralogon groups, and fingerprints. *Mol Pharmacol* (2003) **63**:1256–1272.
299 doi:10.1124/mol.63.6.1256

300 3. Lagerström MC, Schiöth HB. Structural diversity of G protein-coupled receptors and
301 significance for drug discovery. *Nat Rev Drug Discov* (2008) **7**:339–357.
302 doi:10.1038/nrd2518

303 4. Pioszak AA, Xu HE. Molecular recognition of parathyroid hormone by its G protein-
304 coupled receptor. *Proc Natl Acad Sci U S A* (2008) **105**:5034–5039.
305 doi:10.1073/pnas.0801027105

306 5. Grauschopf U, Lilie H, Honold K, Wozny M, Reusch D, Esswein A, Schäfer W,
307 Rücknagel KP, Rudolph R. The N-terminal fragment of human parathyroid hormone
308 receptor 1 constitutes a hormone binding domain and reveals a distinct disulfide
309 pattern. *Biochemistry* (2000) **39**:8878–8887.

310 6. Karpf DB, Arnaud CD, Bambino T, Duffy D, King KL, Winer J, Nissenson RA.
311 Structural properties of the renal parathyroid hormone receptor: hydrodynamic analysis
312 and protease sensitivity. *Endocrinology* (1988) **123**:2611–2620.

313 7. Ehrenmann J, Schöppe J, Klenk C, Rappas M, Kummer L, Doré AS, Plückthun A.
314 High-resolution crystal structure of parathyroid hormone 1 receptor in complex with a
315 peptide agonist. *Nat Struct Mol Biol* (2018) **25**:1086–1092. doi:10.1038/s41594-018-
316 0151-4

317 8. Castro M, Nikolaev VO, Palm D, Lohse MJ, Vilardaga J-P. Turn-on switch in
318 parathyroid hormone receptor by a two-step parathyroid hormone binding mechanism.
319 *Proc Natl Acad Sci U S A* (2005) **102**:16084–16089. doi:10.1073/pnas.0503942102

320 9. Gensure RC, Gardella TJ, Jüppner H. Parathyroid hormone and parathyroid hormone-
321 related peptide, and their receptors. *Biochem Biophys Res Commun* (2005) **328**:666–
322 678. doi:10.1016/j.bbrc.2004.11.069

323 10. Friedman PA. PTH revisited. *Kidney Int Suppl* (2004)S13–S19. doi:10.1111/j.1523-
324 1755.2004.09103.x

325 11. Jüppner H, Abou-Samra AB, Freeman M, Kong XF, Schipani E, Richards J,
326 Kolakowski LF, Hock J, Potts JT, Kronenberg HM. A G protein-linked receptor for
327 parathyroid hormone and parathyroid hormone-related peptide. *Science* (1991)
328 **254**:1024–1026.

329 12. Vilardaga J-P, Romero G, Friedman PA, Gardella TJ. Molecular basis of parathyroid
330 hormone receptor signaling and trafficking: a family B GPCR paradigm. *Cell Mol Life*
331 *Sci* (2011) **68**:1–13. doi:10.1007/s00018-010-0465-9

332 13. Cole JA. Parathyroid hormone activates mitogen-activated protein kinase in opossum
333 kidney cells. *Endocrinology* (1999) **140**:5771–5779. doi:10.1210/endo.140.12.7173

334

335 14. Mahon MJ, Bonacci TM, Divieti P, Smrcka AV. A docking site for G protein βγ
336 subunits on the parathyroid hormone 1 receptor supports signaling through multiple
337 pathways. *Mol Endocrinol* (2006) **20**:136–146. doi:10.1210/me.2005-0169

338 15. Singh ATK, Gilchrist A, Voyno-Yasenetskaya T, Radeff-Huang JM, Stern PH. G
339 alpha12/G alpha13 subunits of heterotrimeric G proteins mediate parathyroid hormone
340 activation of phospholipase D in UMR-106 osteoblastic cells. *Endocrinology* (2005)
341 **146**:2171–2175. doi:10.1210/en.2004-1283

342 16. Malecz N, Bambino T, Bencsik M, Nissenson RA. Identification of phosphorylation
343 sites in the G protein-coupled receptor for parathyroid hormone. Receptor
344 phosphorylation is not required for agonist-induced internalization. *Mol Endocrinol*
345 (1998) **12**:1846–1856.

346 17. Gesty-Palmer D, Chen M, Reiter E, Ahn S, Nelson CD, Wang S, Eckhardt AE, Cowan
347 CL, Spurney RF, Luttrell LM, et al. Distinct beta-arrestin- and G protein-dependent
348 pathways for parathyroid hormone receptor-stimulated ERK1/2 activation. *J Biol Chem*
349 (2006) **281**:10856–10864. doi:10.1074/jbc.M513380200

350 18. Schwindinger WF, Fredericks J, Watkins L, Robinson H, Bathon JM, Pines M, Suva
351 LJ, Levine MA. Coupling of the PTH/PTHrP receptor to multiple G-proteins. Direct
352 demonstration of receptor activation of Gs, Gq/11, and Gi(1) by [alpha-32P]GTP-
353 gamma-azidoanilide photoaffinity labeling. *Endocrine* (1998) **8**:201–209.
354 doi:10.1385/ENDO:8:2:201

355 19. Jilka RL. Molecular and cellular mechanisms of the anabolic effect of intermittent
356 PTH. *Bone* (2007) **40**:1434–1446. doi:10.1016/j.bone.2007.03.017

357 20. Lee M, Partridge NC. Parathyroid hormone signaling in bone and kidney. *Curr Opin*
358 *Nephrol Hypertens* (2009) **18**:298–302. doi:10.1097/MNH.0b013e32832c2264

359 21. Whitfield JF, Morley P, Willick GE, Ross V, Barbier JR, Isaacs RJ, Ohannessian-Barry
360 L. Stimulation of the growth of femoral trabecular bone in ovariectomized rats by the
361 novel parathyroid hormone fragment, hPTH-(1-31)NH2 (Ostabolin). *Calcif Tissue Int*
362 (1996) **58**:81–87.

363 22. Yang D, Singh R, Divieti P, Guo J, Bouxsein ML, Bringhurst FR. Contributions of
364 parathyroid hormone (PTH)/PTH-related peptide receptor signaling pathways to the
365 anabolic effect of PTH on bone. *Bone* (2007) **40**:1453–1461.
366 doi:10.1016/j.bone.2007.02.001

367 23. Hilliker S, Wergedal JE, Gruber HE, Bettica P, Baylink DJ. Truncation of the amino
368 terminus of PTH alters its anabolic activity on bone in vivo. *Bone* (1996) **19**:469–477.

369 24. Gesty-Palmer D, Flannery P, Yuan L, Corsino L, Spurney R, Lefkowitz RJ, Luttrell
370 LM. A beta-arrestin-biased agonist of the parathyroid hormone receptor (PTH1R)
371 promotes bone formation independent of G protein activation. *Sci Transl Med* (2009)
372 **1**:1ra1. doi:10.1126/scitranslmed.3000071

373 25. Potts JT. Parathyroid hormone: past and present. *J Endocrinol* (2005) **187**:311–325.
374 doi:10.1677/joe.1.06057

375 26. Klenk C, Schulz S, Calebiro D, Lohse MJ. Agonist-regulated cleavage of the
376 extracellular domain of parathyroid hormone receptor type 1. *J Biol Chem* (2010)
377 **285**:8665–8674. doi:10.1074/jbc.M109.058685

378 27. Lupp A, Klenk C, Röcken C, Evert M, Mawrin C, Schulz S. Immunohistochemical
379 identification of the PTHR1 parathyroid hormone receptor in normal and neoplastic
380 human tissues. *Eur J Endocrinol* (2010) **162**:979–986. doi:10.1530/EJE-09-0821

381 28. Klenk C, Vetter T, Zürn A, Vilardaga J-P, Friedman PA, Wang B, Lohse MJ.
382 Formation of a ternary complex among NHERF1, beta-arrestin, and parathyroid
383 hormone receptor. *J Biol Chem* (2010) **285**:30355–30362.
384 doi:10.1074/jbc.M110.114900

385 29. Emami-Nemini A, Gohla A, Urlaub H, Lohse MJ, Klenk C. The guanine nucleotide
386 exchange factor Vav2 is a negative regulator of parathyroid hormone receptor/Gq
387 signaling. *Mol Pharmacol* (2012) **82**:217–225. doi:10.1124/mol.112.078824

388 30. Kumar S, Ratnikov BI, Kazanov MD, Smith JW, Cieplak P. CleavPredict: A Platform
389 for Reasoning about Matrix Metalloproteinases Proteolytic Events. *PLoS ONE* (2015)
390 **10**:e0127877. doi:10.1371/journal.pone.0127877

391 31. Zhao L-H, Ma S, Sutkeviciute I, Shen D-D, Zhou XE, de Waal PW, Li C-Y, Kang Y,
392 Clark LJ, Jean-Alphonse FG, et al. Structure and dynamics of the active human
393 parathyroid hormone receptor-1. *Science* (2019) **364**:148–153.
394 doi:10.1126/science.aav7942

395 32. Hakalahti AE, Vierimaa MM, Lilja MK, Kumpula E-P, Tuusa JT, Petäjä-Repo UE.
396 Human beta1-Adrenergic Receptor Is Subject to Constitutive and Regulated N-terminal
397 Cleavage. *J Biol Chem* (2010) **285**:28850–28861. doi:10.1074/jbc.M110.149989

398 33. Kozuka M, Ito T, Hirose S, Lodhi KM, Hagiwara H. Purification and characterization
399 of bovine lung endothelin receptor. *J Biol Chem* (1991) **266**:16892–16896.

400 34. Grantcharova E, Furkert J, Reusch HP, Krell H-W, Papsdorf G, Beyermann M,
401 Schulein R, Rosenthal W, Oksche A. The extracellular N terminus of the endothelin B
402 (ETB) receptor is cleaved by a metalloprotease in an agonist-dependent process. *J Biol*
403 *Chem* (2002) **277**:43933–43941. doi:10.1074/jbc.M208407200

404 35. Couet J, Sar S, Jolivet A, Hai MT, Milgrom E, Misrahi M. Shedding of human
405 thyrotropin receptor ectodomain. Involvement of a matrix metalloprotease. *J Biol*
406 *Chem* (1996) **271**:4545–4552.

407 36. Kaczur V, Puskas LG, Nagy ZU, Miled N, Rebai A, Juhasz F, Kupihar Z, Zvara A,
408 Hackler L, Farid NR. Cleavage of the human thyrotropin receptor by ADAM10 is
409 regulated by thyrotropin. *J Mol Recognit* (2007) **20**:392–404. doi:10.1002/jmr.851

410 37. Boire A, Covic L, Agarwal A, Jacques S, Sherifi S, Kuliopulos A. PAR1 is a matrix
411 metalloprotease-1 receptor that promotes invasion and tumorigenesis of breast cancer
412 cells. *Cell* (2005) **120**:303–313. doi:10.1016/j.cell.2004.12.018

413 38. Ludeman MJ, Zheng YW, Ishii K, Coughlin SR. Regulated shedding of PAR1 N-
414 terminal exodomain from endothelial cells. *J Biol Chem* (2004) **279**:18592–18599.
415 doi:10.1074/jbc.M310836200

416 39. Vallon M, Essler M. Proteolytically processed soluble tumor endothelial marker (TEM)
417 5 mediates endothelial cell survival during angiogenesis by linking integrin
418 alpha(v)beta3 to glycosaminoglycans. *J Biol Chem* (2006) **281**:34179–34188.
419 doi:10.1074/jbc.M605291200

420 40. Mattila SO, Tuhkanen HE, Lackman JJ, Konzack A, Morató X, Argerich J, Saftig P,
421 Ciruela F, Petäjä-Repo UE. GPR37 is processed in the N-terminal ectodomain by
422 ADAM10 and furin. *FASEB J* (2021) **35**:e21654. doi:10.1096/fj.202002385RR

423 41. Mattila SO, Tuusa JT, Petäjä-Repo UE. The Parkinson's-disease-associated receptor
424 GPR37 undergoes metalloproteinase-mediated N-terminal cleavage and ectodomain
425 shedding. *J Cell Sci* (2016) **129**:1366–1377. doi:10.1242/jcs.176115

42. Luttrell LM, Maudsley S, Bohn LM. Fulfilling the Promise of "Biased" G Protein-Coupled Receptor Agonism. *Mol Pharmacol* (2015) **88**:579–588. doi:10.1124/mol.115.099630

43. Kenakin TP. New concepts in pharmacological efficacy at 7TM receptors: IUPHAR review 2. *Br J Pharmacol* (2013) **168**:554–575. doi:10.1111/j.1476-5381.2012.02223.x

44. Onaran HO, Rajagopal S, Costa T. What is biased efficacy? Defining the relationship between intrinsic efficacy and free energy coupling. *Trends Pharmacol Sci* (2014) **35**:639–647. doi:10.1016/j.tips.2014.09.010

45. Bisello A, Chorev M, Rosenblatt M, Monticelli L, Mierke DF, Ferrari SL. Selective ligand-induced stabilization of active and desensitized parathyroid hormone type 1 receptor conformations. *J Biol Chem* (2002) **277**:38524–38530. doi:10.1074/jbc.M202544200

46. Takasu H, Gardella TJ, Luck MD, Potts JT, Bringhurst FR. Amino-terminal modifications of human parathyroid hormone (PTH) selectively alter phospholipase C signaling via the type 1 PTH receptor: implications for design of signal-specific PTH ligands. *Biochemistry* (1999) **38**:13453–13460.

47. Jouishomme H, Whitfield JF, Chakravarthy B, Durkin JP, Gagnon L, Isaacs RJ, Maclean S, Neugebauer W, Willick G, Rixon RH. The protein kinase-C activation domain of the parathyroid hormone. *Endocrinology* (1992) **130**:53–60. doi:10.1210/endo.130.1.1727720

48. Azarani A, Goltzman D, Orlowski J. Structurally diverse N-terminal peptides of parathyroid hormone (PTH) and PTH-related peptide (PTHRP) inhibit the Na+/H+ exchanger NHE3 isoform by binding to the PTH/PTHRP receptor type I and activating distinct signaling pathways. *J Biol Chem* (1996) **271**:14931–14936.

49. Wheatley M, Wootten D, Conner MT, Simms J, Kendrick R, Logan RT, Poyner DR, Barwell J. Lifting the lid on GPCRs: the role of extracellular loops. *Br J Pharmacol* (2012) **165**:1688–1703. doi:10.1111/j.1476-5381.2011.01629.x

50. White AD, Fang F, Jean-Alphonse FG, Clark LJ, An H-J, Liu H, Zhao Y, Reynolds SL, Lee S, Xiao K, et al. Ca2+ allostery in PTH-receptor signaling. *Proc Natl Acad Sci U S A* (2019) **116**:3294–3299. doi:10.1073/pnas.1814670116

51. Li M, Li M, Guo J. Molecular Mechanism of Ca2+ in the Allosteric Regulation of Human Parathyroid Hormone Receptor-1. *J Chem Inf Model* (2021) doi:10.1021/acs.jcim.1c00471

52. Mitra N, Liu Y, Liu J, Serebryany E, Mooney V, Devree BT, Sunahara RK, Yan ECY. Calcium-dependent ligand binding and G-protein signaling of family B GPCR parathyroid hormone 1 receptor purified in nanodiscs. *ACS Chem Biol* (2013) **8**:617–625. doi:10.1021/cb300466n

53. Koth CM, Murray JM, Mukund S, Madjidi A, Minn A, Clarke HJ, Wong T, Chiang V, Luis E, Estevez A, et al. Molecular basis for negative regulation of the glucagon receptor. *Proc Natl Acad Sci U S A* (2012) **109**:14393–14398. doi:10.1073/pnas.1206734109

54. Liang Y-L, Khoshouei M, Deganutti G, Glukhova A, Koole C, Peat TS, Radjainia M, Plitzko JM, Baumeister W, Miller LJ, et al. Cryo-EM structure of the active, Gs-protein complexed, human CGRP receptor. *Nature* (2018) **561**:492–497. doi:10.1038/s41586-018-0535-y

472 55. Dal Maso E, Glukhova A, Zhu Y, García-Nafría J, Tate CG, Atanasio S, Reynolds CA,
473 Ramírez-Aportela E, Carazo J-M, Hick CA, et al. The Molecular Control of Calcitonin
474 Receptor Signaling. *ACS Pharmacology & Translational Science* (2019) **2**:31–51.
475 doi:10.1021/acsptsci.8b00056

476 56. Liang Y-L, Khoshouei M, Glukhova A, Furness SGB, Zhao P, Clydesdale L, Koole C,
477 Truong TT, Thal DM, Lei S, et al. Phase-plate cryo-EM structure of a biased agonist-
478 bound human GLP-1 receptor–Gs complex. *Nature* (2018) **68**:954.
479 doi:10.1002/jcc.20084

480 57. Lei S, Clydesdale L, Dai A, Cai X, Feng Y, Yang D, Liang Y-L, Koole C, Zhao P,
481 Coudrat T, et al. Two distinct domains of the glucagon-like peptide-1 receptor control
482 peptide-mediated biased agonism. *J Biol Chem* (2018) **293**:9370–9387.
483 doi:10.1074/jbc.RA118.003278

484 58. Sarkar K, Joedicke L, Westwood M, Burnley R, Wright M, McMillan D, Byrne B.
485 Modulation of PTH1R signaling by an ECD binding antibody results in inhibition of β-
486 arrestin 2 coupling. *Sci Rep* (2019) **9**:14432. doi:10.1038/s41598-019-51016-z

487 59. Clark LJ, Clark LJ, Krieger J, Krieger J, White AD, White AD, Bondarenko V,
488 Bondarenko V, Lei S, Lei S, et al. Allosteric interactions in the parathyroid hormone
489 GPCR–arrestin complex formation. *Nat Chem Biol* (2020) **42**:946.
490 doi:10.1007/s13361-011-0261-2

491 60. Christopoulos A, Christopoulos G, Morfis M, Udawela M, Laburthe M, Couvineau A,
492 Kuwasako K, Tilakaratne N, Sexton PM. Novel receptor partners and function of
493 receptor activity-modifying proteins. *J Biol Chem* (2003) **278**:3293–3297.
494 doi:10.1074/jbc.C200629200

495 61. Nemec K, Schihada H, Kleinau G, Zabel U, Grushevskyi EO, Scheerer P, Lohse MJ,
496 Maiellaro I. Functional modulation of PTH1R activation and signalling by RAMP2.
497 *bioRxiv* (2021)2021.12.08.471790. doi:10.1101/2021.12.08.471790

498 62. Schechter I, Berger A. On the size of the active site in proteases. I. Papain. *Biochem*
499 *Biophys Res Commun* (1967) **27**:157–162. doi:10.1016/j.bbrc.2012.08.015

500 # Tables

501 **Table 1 – Computational cleavage site prediction of PTH1R ECD.** The sequence of the
502 mature PTH1R ECD (amino acids 23-177) was analyzed for MMP cleavage sites with
503 CleavPredict (30) using position weight matrices for 11 MMPs (MMP-2, MMP-3, MMP-8,
504 MMP-9, MMP-13, MMP-14, MMP-15, MMP-16, MMP-17, MMP-24, MMP-25). For each
505 cleavage site, the residue number of P1, the sequence corresponding to P5-P5' (numbering
506 according to Schechter and Berger (62)) and the position weight matrix score (PWM score)
507 for each MMP subtype are given.

P1 position	residues (P5-P5')	MMP										
		2	3	8	9	10	14	15	16	17	24	25
30	VDADD↓VMTKE											1.32
37	TKEEQ↓IFLLH											0.19
40	EQIFL↓LHRAQ		3.46			2.19				3.43		1.50
46	HRAQA↓QCEKR									2.37		1.71
51	QCEKR↓LKEVL											
61	QRPAS↓IMESD	6.75	8.76	6.13	5.72	8.26	7.60	5.37	7.00	3.42	7.88	5.82
80	GKPRK↓DKASG	1.36										
86	KASGK↓LYPES			1.63				1.31		2.44		4.71
100	EAPTG↓SRYRG				2.52							
102	PTGSR↓YRGRP			1.90								
114	PEWDH↓ILCWP							2.62				
125	GAPGE↓VVAVP	3.56	3.14	2.03								0.21
134	PCPDY↓IYDFN			2.48		1.64		5.02				4.48
137	DYIYD↓FNHKG			2.06								
144	HKGHA↓YRRCD			2.67							0.81	
155	NGSWE↓LVPGH			5.18						2.47		4.00
160	LVPGH↓NRTWA	2.05					1.74	2.03	1.35			
166	RTWAN↓YSECV						1.97		2.16			
173	ECVKF↓LTNET			3.15	6.44		1.30		2.98	3.50		4.39

508

509 **Table 2 – Effects of ECD cleavage on cAMP generation and IP accumulation.** PTH-
510 induced E_{max} values for cAMP and IP generation of $PTH1R^{56-63A}$ or $PTH1R^{72-79A.}$ were
511 compared against that of PTH1R using unpaired t tests. Data summarize results of 3-5
512 independent experiments.

	Difference vs. PTH1R, cAMP (%)			Difference vs. PTH1R, [^{3}H] IP (%)		
	Mean ± SEM	95% C.I.	*p*	Mean ± SEM	95% C.I.	*p*
$PTH1R^{56-63A}$	-37.3 ± 5.9	-52.7 to -21.9	0.0015	35.3 ± 10.7	10.6 to 60.1	0.011
$PTH1R^{72-79A}$	-1.9 ± 1.3	-5.3 to 1.5	0.21	-5.6 ± 19.4	-48.8 to 37.6	0.78

C.I., confidence interval

513

514 **Figures**

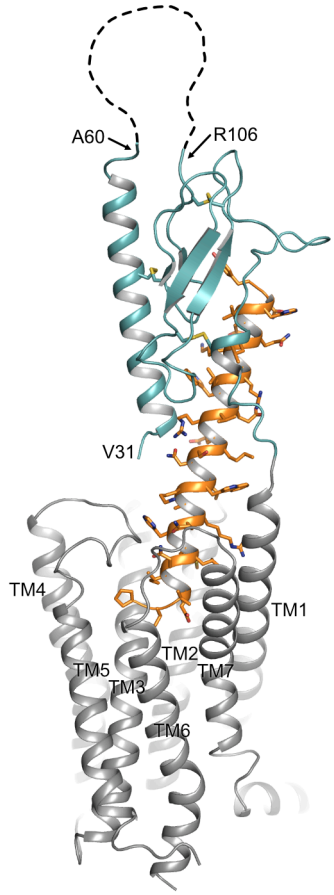

515

516 **Figure 1 – Topology of PTH1R.** Structure of the human PTH1R (transmembrane domain,
517 grey; ECD, teal) in complex with a PTH analog (orange) (PDB ID: 6FJ3). Unstructured
518 residues 61-105 of ECD loop 1 are depicted as a dashed line. The receptor N-terminal residue
519 (V^{31}, as resolved in the crystal structure), residues embracing ECD loop1, and transmembrane
520 helices (TM1-7) are indicated.

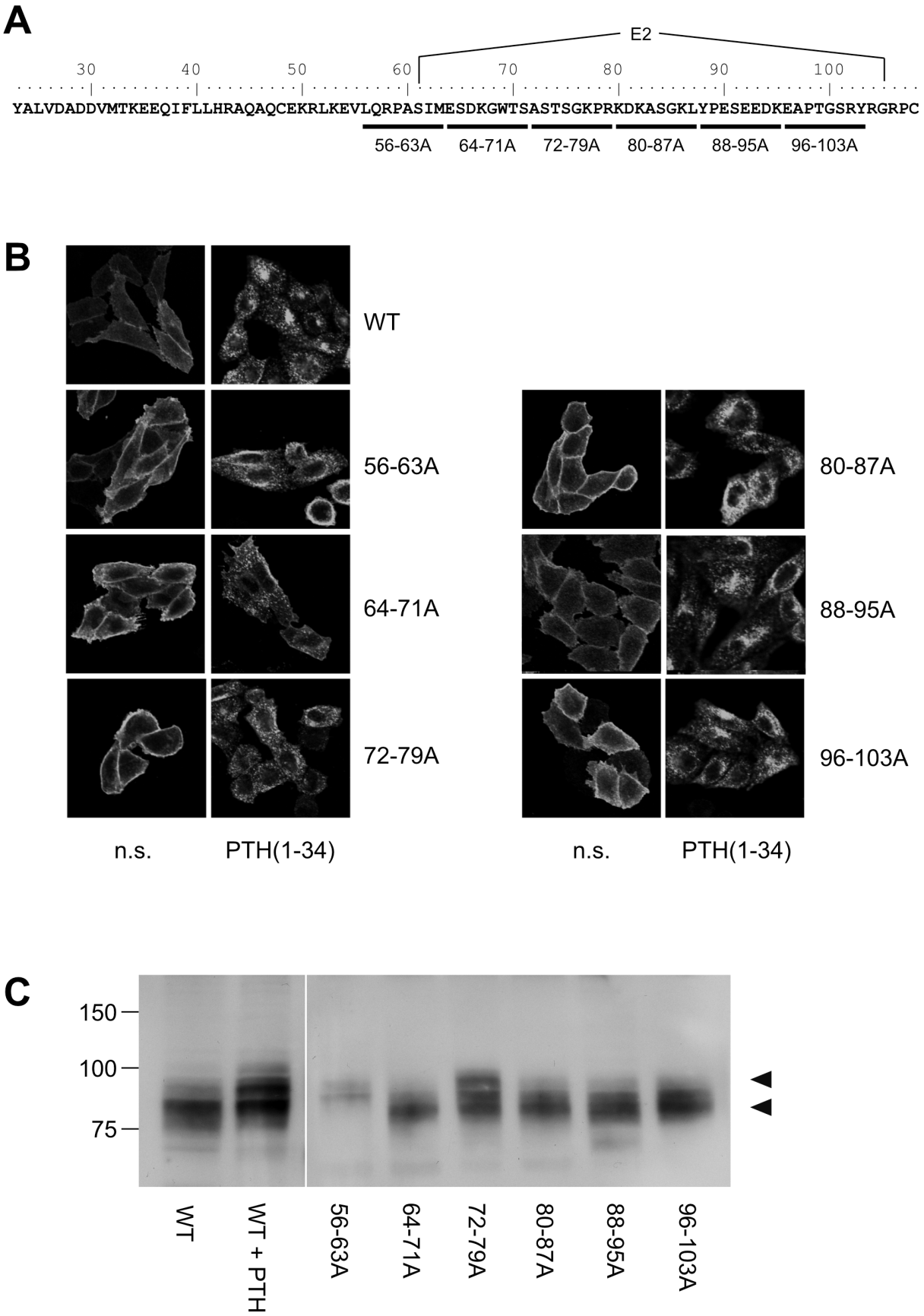
A
E2
30 40 50 60 70 80 90 100
YALVDADDVMTKEEQIFLLHRAQAQCEKRLKEVLQRPASIMESDKGWTSASTSGKPRKDKASGKLYPESEEDKEAPTGSRYRGRPC
56-63A
64-71A
72-79A
80-87A
88-95A
96-103A
B
WT
56-63A
64-71A
72-79A
80-87A
88-95A
96-103A
n.s.
PTH(1-34)
n.s.
PTH(1-34)
C
150
100
75
WT
WT + PTH
56-63A
64-71A
72-79A
80-87A
88-95A
96-103A

521

522 **Figure 2 – Mapping of the protease cleavage site of PTH1R ECD by alanine scan. (A)**
523 Amino acid sequence of the extracellular domain of the human PTH1R. Stretches of 8 amino
524 acids that were replaced by alanine residues are indicated by horizontal bars. Exon E2 is
525 marked above the sequence. **(B)** CHO cells stably expressing PTHR variants were treated
526 with 100 nM PTH(1-34) for 30 min or left untreated. Subsequently, cells were fixed,
527 permeabilized, and stained with rabbit anti-PTH1R antibody followed by Cy2-labeled anti-
528 rabbit antibody. PTHR was visualized by confocal microscopy. **(C)** CHO cells stably
529 expressing PTHR variants were lysed, and PTH1R was monitored by reducing SDS-PAGE
530 and Western blotting. Cells were treated with 100 nM PTH(1-34) for 12 h prior to cell lysis
531 where indicated. Arrowheads depict the cleaved (MW ~80 kDa) and the uncleaved (MW
532 ~90 kDa) PTH1R band.

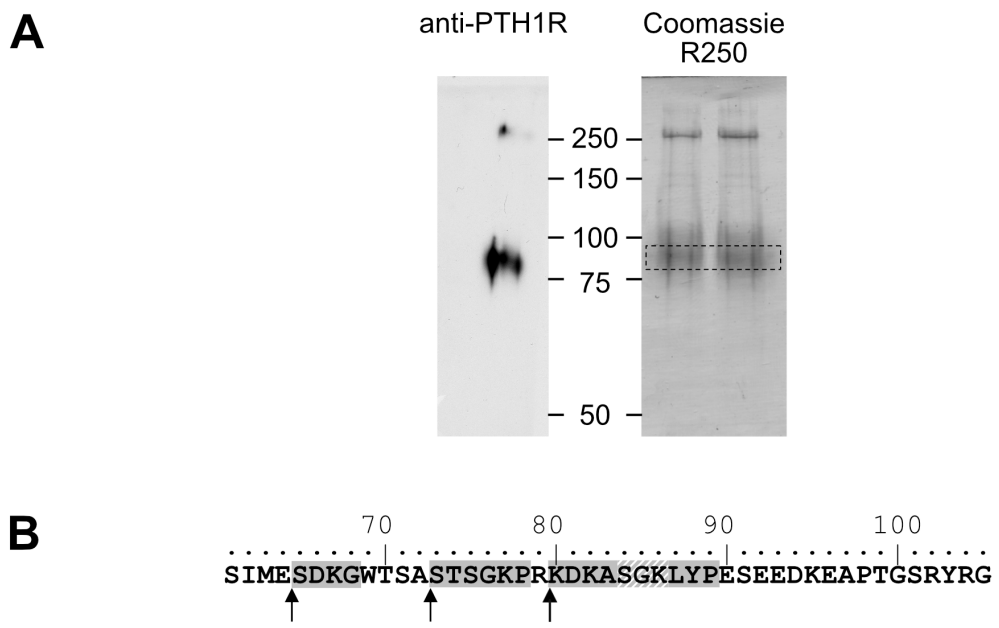

533

534 **Figure 3 – Mapping of the protease cleavage site of PTH1R ECD by N-terminal**
535 **sequencing. (A)** Human PTH1R with C-terminal Strep2-tag was purified from stably
536 expressing CHO cells by two-step affinity purification. A fraction of the purified receptor was
537 subjected to Western blot and probed with anti-PTH1R antibodies (left panel). The remaining
538 purified receptor protein (~50 µg) was transferred on PVDF membranes and stained with
539 Coomassie blue R250. The band corresponding to PTH1R was cut out and subjected to
540 microsequencing (right panel, dashed box). **(B)** Sequence of exon E2 (amino acids 61-105).
541 Sequences obtained from microsequencing are shaded gray. The position of the N-terminal
542 amino acid is marked by an arrow. Residues 84-86 (gray diagonal stripes) were not resolved
543 in the Edman degradation.

544

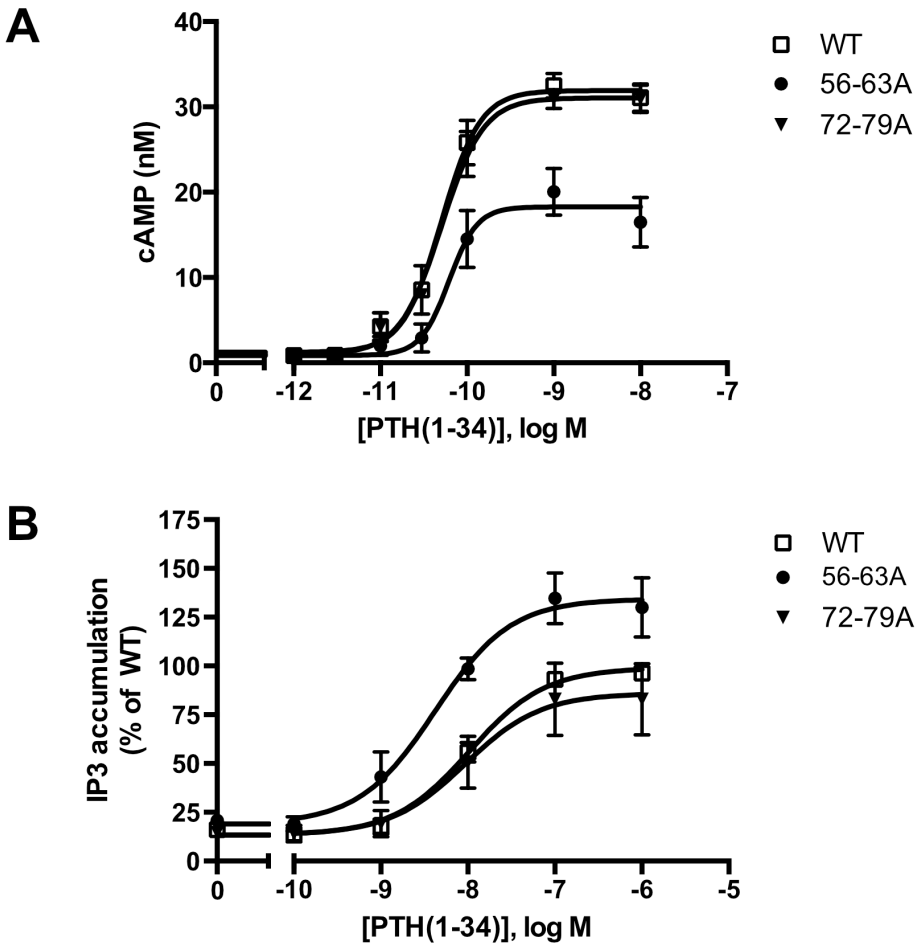

545

546 **Figure 4 – Protease cleavage changes the signaling specificity of PTH1R from G_q and G_s.**
547 **(A)** Flp-In CHO cells stably expressing PTH1R, $PTH1R^{56-63A}$ or $PTH1R^{72-79A}$ were stimulated
548 for 20 min with PTH(1-34) at the indicated concentrations, and cAMP levels were quantified
549 with a radioimmunoassay. The means ± S.E.M. of five independent experiments are shown.
550 **(B)** Flp-In CHO cells stably expressing PTH1R, $PTH1R^{56-63A}$ or $PTH1R^{72-79A}$ were incubated
551 with [*myo*-2-^{3}H(N)]inositol and 0.2% fetal calf serum for 16 h. Cells were stimulated for
552 60 min with the indicated concentrations of PTH, and [^{3}H]IP_3 levels were quantified in a
553 scintillation counter after chromatographic separation. Data represent the means ± S.E.M. of
554 five individual experiments.

555

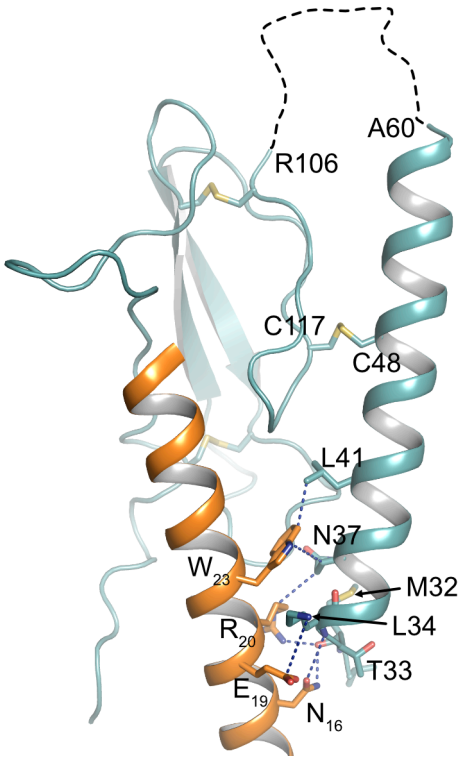

556

557 **Figure 5 – Interface between PTH and α1-helix of PTH1R ECD.** Crystal structure of the
558 PTH1R ECD (teal) in complex with PTH (orange) (PDB ID: 6FJ3). Residues forming the
559 interface are shown as stick, and contacts are indicated as blue dashed lines. The unstructured
560 loop 1 of the ECD is shown as black dashed line.